

Sorption Kinetics of Hydrophobic Organic Compounds to Natural Sediments and Soils

Shian-chee Wu and Philip M. Gschwend*

Ralph M. Parsons Laboratory, Department of Civil Engineering, Massachusetts Institute of Technology, Cambridge, Massachusetts 02139

■ Sorption kinetics of hydrophobic organic chemicals to and from suspended sediment and soil particles is described by a radial diffusive penetration model modified by a retardation factor reflecting microscale partitioning of the sorbate between intraaggregate pore fluids and the solids making up the aggregate grains. In light of this and other sorption kinetics models, a closed-loop-stripping apparatus with a photoionization detector operating in-line was used to examine the effects of sorbate hydrophobicity, sorbent particle size, and system temperature on solid-solution exchange over times of seconds to days. Our results indicate that a single effective diffusivity parameter, which is predictable from compound solution diffusivity, octanol-water partition coefficient, and sorbent organic content, density, and porosity, can be used to quantify the sorption kinetics.

Introduction

Sorption on sediment and soil particles plays a major role in controlling the fate of organic pollutants in aquatic environments. Partitioning models, in which equilibrium between dissolved and sorbed species is assumed, are often adequate to describe transport phenomena, particularly when solid-solution contact times are relatively long (days to months). Examples where equilibrium descriptions appear appropriate include organic compound exchange between slowly settling suspended solids in lakes and rivers and to and from aquifer soils and groundwater percolating at common flow velocities.

However, there is evidence that in some situations sorption/desorption transfers are sufficiently slow as to invalidate the use of equilibrium models. Several investigators evaluating the transport of organic compounds through leached soil columns have found both asymmetric distributions of chemical concentrations vs. depth and nonsigmoid or tailing breakthrough curves (1-4). These observations are best explained by recognizing that the sorptive exchange "reactions" or mass transfers are slow with respect to advective flow of the pore fluids. Investigations of the release of organic pollutants from contaminated sediments also provide evidence for sorptive exchange limiting transport. For example, transfer of phthalates and polychlorinated biphenyls from natural sediments, especially those deposited as fecal pellet aggregates and those exposed to the pollutant for extended times (>months), has been found to occur on time scales of days to months, (5-7). In all of these cases, fluid-solid contact time is short (minutes to days), and mass transfers do not proceed to completion before "new" fluids have displaced incompletely equilibrated "old" fluids. Other situations where sorption kinetics will undoubtedly play a role include the following: storm-derived resuspension of quickly redeposited bed sediments; soils rapidly infiltrated by heavy rains, flooding events, or wastewater applications; sediment-water mixing associated with dredging and dumping operations.

Typical fate and transport models (e.g., SERATRA (8); TOXIWASP (9)) assume local sorption equilibrium in suspensions as well as sediment beds. Such an assumption

may result in significant error in prediction of fate in the aforementioned situations. In order to develop an accurate description of hydrophobic compound transport in aquatic environments where physical-mixing processes expose solids to solutions on time scales similar to or shorter than those of sorption transfers, we must understand the factors controlling sorption kinetics.

Many models have been developed to simulate sorption kinetics. Among them the one-box model is the simplest model in which the sorption rate is a first-order function of concentration difference between the sorbent (viewed as a completely mixed box) and the solution, and is quantified by a single rate constant, k_r (Figure 1) (10, 11). This mathematical formulation implies that sorptive exchange is limited by only one of many conceivably important processes including binding by single class of sorbing site or mass transfer across a boundary. However, the one-box model does not fit experimental data well. Sorption kinetics data always show a rapid initial uptake followed by a slow approach to equilibrium (2, 12, 13; this paper). The improved modeling approach typically utilized involves subdividing the sorbent into two compartments. This conceptualization corresponds to physical situations in which there are two classes of sorbing sites, two chemical reactions in series, or a sorbent with an exterior part (easily accessible) and an inner part (exchanging slowly) (Figure 1). Unfortunately, this type of model retains three independent fitting parameters (i.e., k_1 , the exchange rate from the solution to the first box; k_2 , the exchange rate from the first box to the second box; X_1 , the fraction of total sorbing capacity in the first box) that cannot be easily evaluated or estimated for new combinations of chemicals and solids. Numerous other mass transfer approaches (e.g., those reviewed in ref 14) similarly suffer in having no fundamental basis on which to predict the values of the model parameters.

Therefore, the objective of this work was to develop and experimentally verify a model of sorption kinetics which is based on known physical and chemical processes (i.e., molecular diffusion and phase partitioning) and the commonly available parameters used to describe them.

Physically Based Model for Sorption Kinetics

As a point of departure, we assume that the sediment and soil particles of most concern for hydrophobic organic compound sorption are aggregates of fine mineral grains and natural organic matter. The aggregate nature of natural sorbents as they exist in the environment, including suspended solids (15, 16), sediments (17), and soils (18-20), is well documented. Therefore, following the previous suggestion of Leenheer and Ahlrichs (13) we hypothesize that the kinetics of solution-solid exchange should be described as a radial diffusive penetration of organic pollutants into these porous natural particles. That is, sorbate molecules diffuse through the pore fluids held in the interstices of natural silt aggregates, and their penetration is "retarded" by microscale partitioning of the compounds between essentially mobile (i.e., dissolved in intraparticle pore fluids) and immobile (i.e., in/on intra-

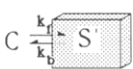
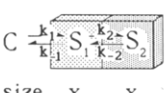

Kinetics Models	Independent Kinetics Fitting Parameters (derived parameters)
One-box model 	k_f $(k_b = k_f / K_p)$
Two-box model  size x_1 x_2	k_1, k_2, x_1 $(k_{-1} = k_1 / K_p)$ $(k_{-2} = k_2)$ $(x_2 = 1 - x_1)$
Diffusion model 	D_{eff}

Figure 1. Comparison of three sorption kinetics models. K_p is the partition coefficient.

particle solids) states of the organic chemical.

This physical conceptualization suggests that the same approaches used to develop intraparticle diffusion models in synthetic particles may be appropriate for natural sorbents. Chemical engineers have long considered intraparticle diffusion to limit sorption of organic compounds by activated carbon, synthetic resins, and porous catalysts (21–24). Similarly, separation scientists have used intraparticle diffusion models to explain chromatographic phenomena (25). Soil scientists have recently demonstrated the effectiveness of this physical view for transport of conservative chemicals through soils in their natural aggregate state (3, 26). For the following model development discussion, derived from the engineering, soil science, and separation science literature, it will be assumed that the sorbents of interest are spherical and internally homogeneous porous media (27). We shall confine our treatment here to instances in which the bulk fluid is sufficiently turbulent that an exterior boundary layer does not limit sorptive exchange.

The time rate of change of sorbed compound per unit volume can be mathematically expressed (28) as

$$\frac{\partial S(r)}{\partial t} = D_m n \left[\frac{\partial^2 C'(r)}{\partial r^2} + \frac{2}{r} \frac{\partial C'(r)}{\partial r} \right] \quad (1)$$

where $S(r)$ is the local total volumetric concentration in porous sorbent (mol/cm^3), $C'(r)$ is the compound concentration free in pore fluid and varying with radial distance (r) (mol/cm^3), n is the porosity of the sorbent (cm^3 of fluid/ cm^3 total), and D_m is the pore fluid diffusivity of the sorbate (cm^2/s). By definition

$$S(r) = (1 - n)\rho_s S'(r) + nC'(r) \quad (2)$$

in which $S'(r)$ is the concentration of the immobile bound state (mol/g) and ρ_s is the specific gravity of the sorbent (g/cm^3). If the pore fluid concentration and the solid-bound concentration are locally in equilibrium, a sorption isotherm relating these states applies, such as

$$S'(r) = K_p C'(r) \quad (3)$$

where K_p is the equilibrium partition coefficient ($(\text{mol}/\text{g})/(\text{mol}/\text{cm}^3)$). The isotherm relationship can be used to restate the intraparticle diffusion kinetics in S only:

$$S(r) = (1 - n)\rho_s K_p C'(r) + nC'(r) = [(1 - n)\rho_s K_p + n]C'(r) \quad (4)$$

$$\frac{\partial S(r)}{\partial t} = \frac{D_m n}{[(1 - n)\rho_s K_p + n]} \left[\frac{\partial^2 S(r)}{\partial r^2} + \frac{2}{r} \frac{\partial S(r)}{\partial r} \right] = D'_{eff} \left[\frac{\partial^2 S(r)}{\partial r^2} + \frac{2}{r} \frac{\partial S(r)}{\partial r} \right] \quad (5)$$

where D'_{eff} is the effective intraparticle diffusivity (cm^2/s). When K_p is large (true for hydrophobic compounds), the effective diffusivity, D'_{eff} , is simply

$$D'_{eff} = \frac{D_m n}{(1 - n)\rho_s K_p} \quad (6)$$

One last consideration is that this model of radial diffusive penetration assumes (1) the entire surface area is available for mass flux and (2) the path length of diffusive transfer is half the particle diameter. Clearly the D'_{eff} appropriate for natural silts must include a correction factor, $f(n, t)$, which is a function of intraaggregate porosity and tortuosity (t), that is

$$\frac{\partial S(r)}{\partial t} = D'_{eff} \left[\frac{\partial^2 S(r)}{\partial r^2} + \frac{2}{r} \frac{\partial S(r)}{\partial r} \right] \quad (7)$$

where

$$D'_{eff} = D'_{eff} \cdot f(n, t)$$

This model of sorption kinetics is quite flexible and physically reasonable. The compound properties (diffusivity in solution and hydrophobicity) and those of the natural sorbents (e.g., organic content, particle size, and porosity) can be used in the model to predict a priori sorption kinetics for each chemical and/or site of interest.

Experimental Section

Materials. Four chlorobenzene congeners (1,4-dichlorobenzene, 1,2,4-trichlorobenzene, 1,2,3,4-tetrachlorobenzene, pentachlorobenzene) were purchased from Foxboro/Analabs Co. (North Haven, CT) and used as received. Milli-Q water (Millipore, Bedford, MA) was used for aqueous preparations.

Three natural sediments and soils were used in our experiments. Sediments taken from river beds were air-dried, sieved through a No. 20 standard sieve (opening = 0.84 mm), and stored at room temperature. Air-dried soil samples provided to us by Dr. S. Karickhoff of the Environmental Research Laboratory, U.S. EPA (Athens, GA), were previously treated similarly. Soil and sediment suspensions used in the kinetics experiments were prepared by adding about 50 mL of water to air-dried sediments or soils 2 days in advance. The suspensions were shaken by hand several times during this 2-day period to facilitate wetting and establishment of a natural aggregation condition.

Some properties of the sediments are listed in Table I. Wet particle sizes were determined by sieving 2 L of sediment suspension prepared 2 days previously and containing 2–3 g of dry sediments through standard sieves (openings: 840, 177, and 88 μm) and Nitex net (openings: 53 and 28 μm). The amount of the smallest size fraction was determined by measuring the total solid mass left in the suspension after the last sieving. The dry solid densities were estimated with the specific gravity bottle me-

Table I. Properties of Sediments and Soils

sample name	source	combustible ^a loss (550 °C, 25 min), %	dry density, g/cm ³	wet particle size distribution fraction by weight at diameter, μm					
				>840	840-177	177-88	88-53	53-28	<28
Charles River sediments	Charles River, MA	17.0	2.25	0.03	0.34	0.14	0.14	0.17	0.18
contaminated Charles River sediments	prepared in our lab	17.7	ND ^c	0.0	0.04	0.12	0.22	0.28	0.34
Iowa soils	EPA (EPA-10)	6.5 ^b	2.6	0.04	0.32	0.15	0.15	0.27	0.08
North River sediments	North River, MA	8.8	2.51	0.01	0.19	0.23	0.18	0.15	0.24
contaminated North River sediments	prepared in our lab	8.4	ND	0.0	0.02	0.06	0.17	0.43	0.32

^aCombustible loss includes organic matter and possibly chemically bound water. The organic carbon content (f_{oc}) will be slightly less than half of combustible loss (20). ^bThe organic carbon content of Iowa soils is 2.1% (Dr. Karickhoff). ^cND = not determined.

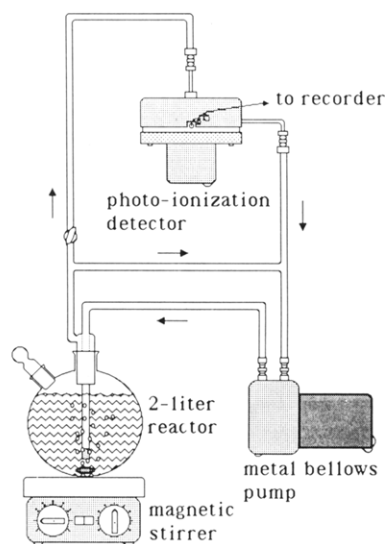


Figure 2. Apparatus for sorption-desorption kinetics experiments.

thod (20). The organic matter content was estimated by heating the sample at 550 °C for 25 min and determining the weight loss (20). Contaminated sediments were prepared by equilibrating an aqueous solution of the test compound with a sediment suspension. Then, sediments were separated from water by settling for 1 week and homogenized by stirring. Water content, size distribution, and combustible loss were measured as well.

Experimental Apparatus. We have developed an apparatus (Figure 2) that enabled us to continuously monitor the changing dissolved concentrations of hydrophobic sorbates on time scales of seconds to days without performing solid-solution phase separations which often lead to analytical difficulties (29). The setup included a 2-L reaction vessel which was continuously stirred with a magnetic stirrer. During periods of analysis, stripping air was pumped with a flow rate of 90 cm³/s by a stainless steel bellows pump (MB-21, Metal Bellows Co., Sharon, MA) and recycled in a closed-loop all-glass system except that a small part of the flow was diverted through a parallel loop containing a photoionization detector, PID (PI-52-02, HNU Systems Inc., Newton, MA). The PID measured the chemical concentration in the gas phase, thereby reflecting the activity of the dissolved compound in the solid suspension. With small headspace volume (0.1 of suspension volume) and Henry's law constants of 0.1–0.15 ((mol/cm³ of air)/(mol/cm³ of water)) for the compounds studied, this apparatus could respond to changes in solution concentration with a rate constant of 4 min⁻¹ (i.e., 50% to equilibrium in 10 s) and could be used up to 48 h without noticeable loss of compounds (e.g., due to leaks or decomposition by the PID). The temperature of the solution was maintained at room temperature (25 ± 3 °C) with a hot plate. The loop of flow containing the detector was

switched to an identical reference system with only water (not shown in Figure 2) in order to check the base-line detector response from time to time.

Experimental Procedure for Sorption and Desorption Kinetics. At the beginning of a sorption kinetics experiment only water and clean air were in the experimental system. The responses of the reaction system and the reference system were recorded. In order to dissolve the test compound into the water and avoid inclusion of microscopic crystals in the solution, a small crystal of the compound which had been weighed on a Cahn 25 microbalance (Cahn Instruments, Inc., Cerritos, CA) was placed within a bolus of glass wool or carefully melted and recrystallized onto the glass wall of a removable section of tubing of the stripper in the gas path before the bubbler. By recirculation of the air through the stripper, the crystal sublimed and the compound was transferred to the aqueous solution within 2 days if the amount put in was smaller than the amount necessary to saturate the solution. If the solution became saturated, the remaining crystalline compound was removed, and the concentration in the solution was lowered to 50% of the saturated concentration by stripping with clean air and monitoring the gas phase with the PID.

The sorption experiment was initiated by pouring about 50 mL of sediment or soil suspension into the side mouth of the reaction vessel. Tests showed that opening the side mouth for several seconds did not result in significant loss of compound from the system. The activity of the compound in the solution was monitored continuously during the first hour and was measured intermittently afterward. Typically, there was no measurable change of activity after 1 or 2 days. Therefore, the experiments lasted 2 or 3 days, and the last measured activity was assumed to be the equilibrium activity at infinite time. Desorption experiments were similar to sorption experiments except that contaminated sediments were poured into clean water in the reactor.

Since the size of the particle aggregates was expected to be a critical factor in controlling sorptive exchange, we examined the particle size distributions of Charles River sediments under continuous bubbling and stirring for different time periods. The results show that the particle size distribution shifted significantly to smaller sizes with combined bubbling and stirring (Figure 3). Therefore, sorption rates would be continuously increased throughout the experiment by shortening the diffusion path and increasing particle surface area. This phenomenon was observed in our early experiments (i.e., experiments 1 and 4–6) in which the suspensions were bubbled throughout the experimental periods and the time to reach sorption equilibrium was relatively long. Consequently, we modified our subsequent experimental procedure so that continuous bubbling was used only for the first hour, and then limited to brief periods necessary to monitor the sorption progress at longer times. This procedure lowered the energy input

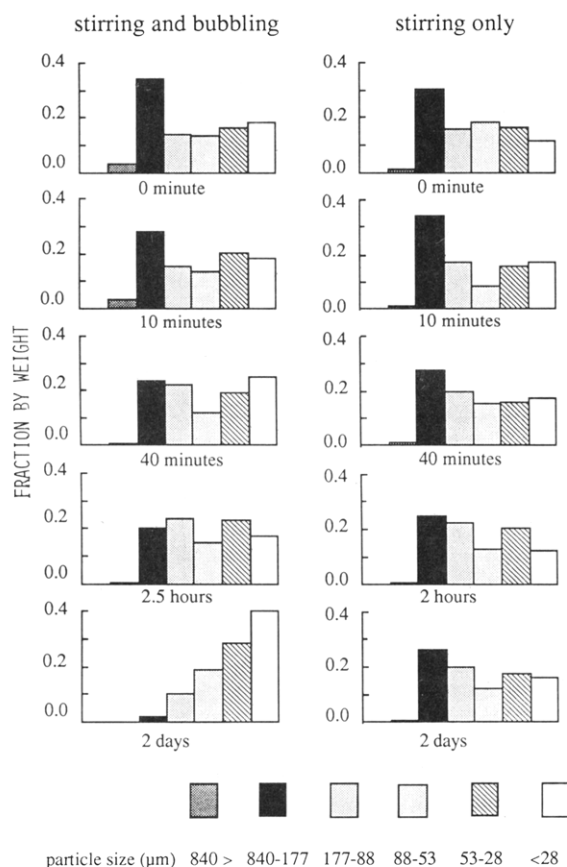


Figure 3. Particle size distributions of Charles River sediments during (left) continuous bubbling and stirring or (right) continuous stirring only.

into the sediment suspension by about 90% and therefore greatly reduced the shearing, causing particle disaggregation. Thus, when we observe the size distribution for 2 days of continuous stirring (Figure 3), we observe much more stable particle size distributions.

Model Simulation

In order to evaluate the effectiveness of the radial diffusion model, model simulations were compared with the experimental results. In the intraparticle diffusion governing equation (eq 7), the intraparticle diffusivity, D_{eff} , is the only parameter necessary to quantify the process for the given conditions. The boundary condition at the particle surface (r = particle radius, R) is given by the expression of local equilibrium:

$$S(r = R) = (1 - n)\rho_s K_p C \quad (8)$$

where C is the dissolved concentration in bulk solution. C is not necessarily a constant. In our experimental conditions (i.e., a well-mixed closed system) C can be related to S by a mass conservation equation:

$$\frac{V}{V_s}C + \bar{S} = \frac{V}{V_s}C_0 + \bar{S}_0 \quad (9)$$

in which V and V_s are the total volume of solution and particles, respectively. \bar{S}_0 is the average initial sorbed concentration over all particles. The averaged concentration at any time, \bar{S} , is given by

$$\bar{S} = \sum \left[\frac{3}{4\pi R^3} \int_0^R 4\pi r^2 S(r) dr \right] \quad (10)$$

Analytical solutions are available for this intraparticle diffusion description of sorption kinetics in which all the particles are assumed to be the same size and the exterior

solution volume, V , is well-mixed (28). Analytical solutions, however, are only valid for simple boundary conditions and for a mix of particles having a very narrow size distribution (i.e., the particle sorption behavior can be represented by a single average diameter if the size distribution spans only about 1 order of magnitude (30)). In aquatic environments, the particle sizes of sediments and soils in their natural aggregated state span several orders of magnitude, and open systems in which bulk dissolved concentration varies with time are very common. Therefore, a numerical method was developed in which particles were divided into several size classes and the bulk dissolved concentration was allowed to vary. Individual particles in each size class were divided into a certain number of equal-interval concentric hollow spheres. Derivatives in the governing equation were replaced by finite difference expressions. An explicit Euler method was used for integration in each time step. The element size in each particle class was chosen so that the numerical solution converged to the corresponding analytical solution within 1 min of simulated experimental time which is the lower limit of the time of interest. The details of the numerical method are described further in ref 31.

The best-fit value of D_{eff} was obtained by adjusting the D_{eff} in the model so that the data points at the most rapidly changing section around the midpoint of equilibration, $t_{1/2}$ (i.e., when $(C - C_{\text{equilibrium}})/(C_0 - C_{\text{equilibrium}}) = 0.5$), fell on the predicted curve. This method gives the best results because the predicted curve is very sensitive to the selected D_{eff} at $t_{1/2}$, and the effects of experimental errors at the very beginning and near the end of an experiment where errors are largest can be avoided.

When the time scale of sorption is close to the time scale of the apparatus response ($(\ln 2)/(4 \text{ min}^{-1})$) there will be significant error in the fit values of D_{eff} because what we measured was the true sorption kinetics response superimposed on an apparatus response. By assuming that the apparatus response to changes in solution activity of sorbates can be described with a first-order rate expression and a response rate constant of 4 min^{-1} , we can estimate the extent to which the observed D_{eff} differs from a "true" value. Our worst cases (i.e., shortest time to exchange) involved dichlorobenzene sorption on Charles River ($t_{1/2} = 0.8 \text{ min}$; therefore, $D_{\text{eff,obsd}} \approx 1.48D_{\text{eff,true}}$) and trichlorobenzene on the same sediments ($t_{1/2} = 1.6 \text{ min}$; therefore, $D_{\text{eff,obsd}} \approx 1.16D_{\text{eff,true}}$). Apparatus response errors are insignificant ($<1\%$) for our other experimental results.

Results and Discussion

The experimental conditions and results are summarized in Table II and are shown in the following figures. The ratio of $C - C_e$ to $C_0 - C_e$ is plotted in most figures to magnify the concentration change in solution. Two experiments (Figure 4) that were performed with the same compound and sediments and similar initial conditions show the reproducibility of this experimental protocol.

Evidence for Intraparticle Diffusion. The results show several very interesting features of sorption consistent with the intraparticle diffusion model. First, large particles show a slower sorption approach to equilibrium than otherwise similar smaller particles when we use the same sorbate (Figure 5). When these same sediments are disaggregated (i.e., by sonication) before sorption experiments, they demonstrate an even faster uptake rate. Clearly by reducing the diffusive path length into the interior of the particles and by increasing the exposed sorbent surface area, we can greatly increase sorption rates.

Second, compounds with greater hydrophobicity (i.e., higher K_{ow}) have slower uptake rates into the same sedi-

Table II. Experimental and Model Simulation Results

expt no.	Figure	sorbate ^a	C ₀ , μM	C _e /C ₀	sorbent ^b	solid concn, ρ, mg/L	particle size, μm	temp, °C	K _p , cm ³ /g	D _{eff} ^c , cm ² /s
Sorption										
1	5	P	2.0	0.48	CR	235	mixed	23	4690	<8.3 × 10 ⁻¹¹ d
2	10a	TR	13.7	0.29	CR	9350	mixed	24	265	3.3 × 10 ⁻¹⁰
3	10a	D	4.4	0.39	CR	17900	mixed	22	87	1.0 × 10 ⁻⁹
4	5	TE	1.4	0.46	CR	968	mixed	24	1220	<2.0 × 10 ⁻¹⁰ d
5	4	TE	3.2	0.39	CR	1030	96	23	1520	<2.5 × 10 ⁻¹⁰ d
6	4	TE	3.7	0.62	CR	442	232	28	1390	<3.3 × 10 ⁻¹⁰ d
7	6	TE	2.5	0.58	CR	1060	mixed	55	684	<4.2 × 10 ⁻¹⁰ d
8	6	TE	2.3	0.44	CR	1240	mixed	40	1020	<4.2 × 10 ⁻¹⁰ d
9	10b	TE	2.8	0.63	IS	10200	mixed	22	58	1.0 × 10 ⁻⁹
10	10b	P	1.6	0.5	IS	4250	mixed	25	239	2.5 × 10 ⁻¹⁰
11	10c	TE	2.5	0.54	NR	2050	mixed	23	418	5.0 × 10 ⁻¹¹
12	10c	P	0.4	0.45	NR	770	mixed	26	1560	8.3 × 10 ⁻¹²
Desorption										
13	10d	TE	0.0		CR	2270	mixed	27	1220 ^e	8.3 × 10 ⁻¹¹
14	10d	TE	0.0		NR	2390	mixed	24	418 ^e	1.3 × 10 ⁻¹⁰

^aP, pentachlorobenzene; TE, 1,2,3,4-tetrachlorobenzene; TR, 1,2,4-trichlorobenzene; D, 1,4-dichlorobenzene. ^bCR, Charles River sediments; IS, Iowa soils; NR, North River sediments. ^cK_p's of sorption cases were calculated from the observed dissolved concentration at the end of the kinetics experiments. K_p's of desorption cases were taken as the same as the K_p's of corresponding sorption cases. ^dThe D_{eff}'s in these model simulation results are upper limits because of an artificially higher uptake rate caused by bubbling-derived particle breakage. ^eFrom model fits of kinetics data.

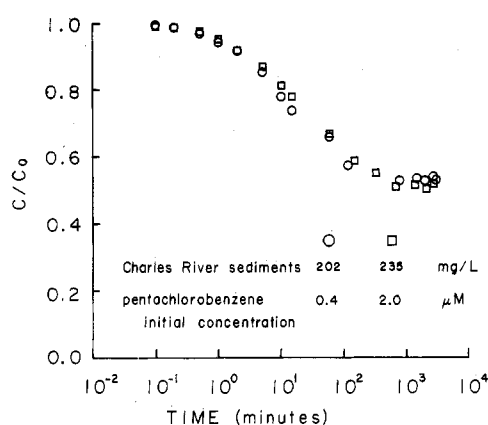


Figure 4. Experimental results of two similar treatments showing reproducibility of the experimental protocol for sorption kinetics.

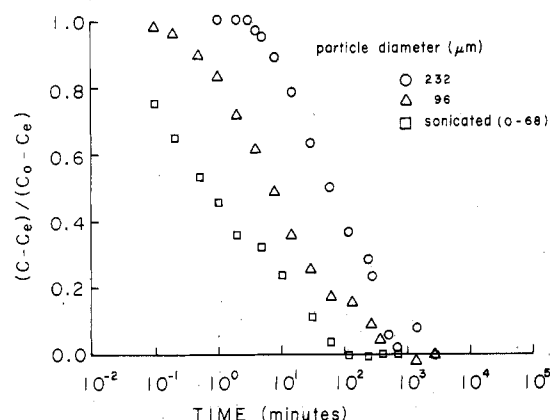


Figure 5. Sorption kinetics experimental results for tetrachlorobenzene on Charles River sediments with two different particle sizes and the same sediments disaggregated by sonication.

ments (Figure 6; K_{ow} from ref 32). This corroborates the previous results of Karickhoff (12), who studied polycyclic aromatic hydrocarbons. This finding is important, because if local sorption equilibrium between molecules dissolved in pore fluids and those sorbed locally in the aggregates is always established, the chemicals with higher partition coefficients are predicted to penetrate the natural sorbent

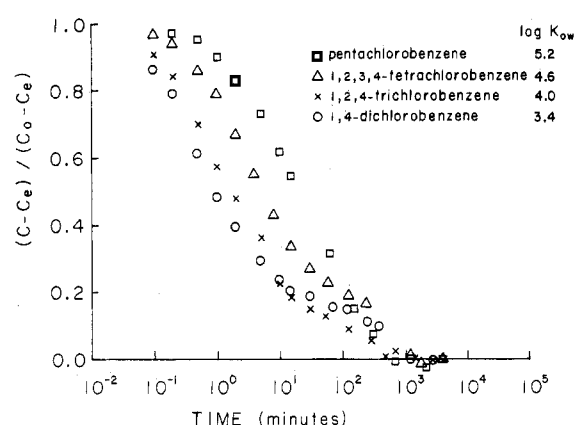


Figure 6. Comparison of sorption kinetics experimental results for four chlorobenzene congeners exhibiting a range of hydrophobicities (K_{ow} from ref 32) on Charles River sediments.

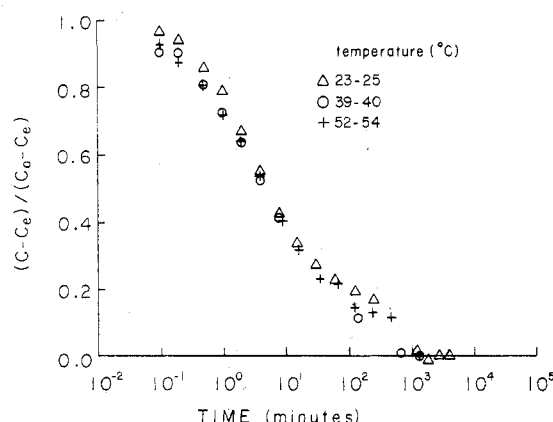


Figure 7. Comparison of sorption kinetics experimental results for tetrachlorobenzene on Charles River sediments at three different temperatures.

aggregates more slowly if diffusive transport occurs primarily in the intraparticle pore fluids. The compounds with higher molecular weight (also higher K_{ow} in this case) will penetrate slower because of lower diffusivities. Since molecular diffusivity is inversely proportional to one-third power of molar volume (33), differences in the solution

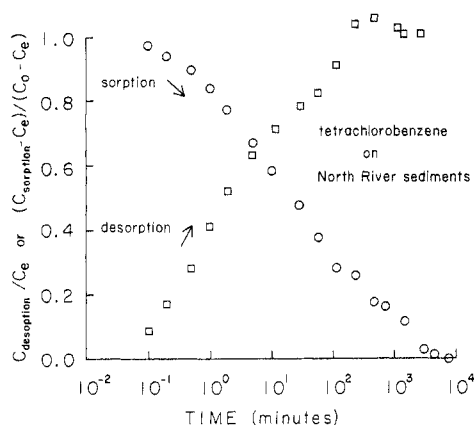


Figure 8. Desorption vs. sorption kinetics for tetrachlorobenzene on North River sediments.

diffusivities do not vary greatly among these four compounds. Therefore, the effects of hydrophobicity dominate the variation of sorption rate for the different compounds.

Finally, over a temperature range of 30 °C, there is no large change in sorption rates (Figure 7). The temperature could potentially affect the sorption rate in two ways in terms of intraparticle diffusion. First, diffusivities in solution and pore water vary directly with temperature. However, a temperature change of 30 °C corresponds to only about a 10% range in molecular diffusivities (33), and we do not believe our observations are sufficiently precise to show this. Second, temperature can change the partition coefficients and consequently change the effective diffusivities which determine the sorption rates. The sorption partition coefficient of tetrachlorobenzene to Charles River sediments is indeed smaller at 55 °C ($K_p = 0.68 \times 10^3 \text{ cm}^3/\text{g}$) than at 40 °C ($K_p = 1.0 \times 10^3 \text{ cm}^3/\text{g}$) and at 24 °C ($K_p = 1.2 \times 10^3 \text{ cm}^3/\text{g}$) (Table II). This relationship between the partition coefficients and the temperature corresponds to an exothermic sorption heat of about -3.5 kcal/mol (derived from the Gibbs-Helmholtz equation; see ref 34). Given the observed temperature effect on K_p , we predict from eq 6 the effective diffusivity to vary by a factor of 2 in these experiments. As shown in Table II and as will be discussed, the effective diffusivities needed for model simulations to fit the data for this range of temperatures varied by about this magnitude.

The desorption experiments further confirmed that the reversible processes of intraparticle diffusion and phase partitioning (29, 35) may be used to quantify solid-to-solution exchange kinetics. As can be seen in Figure 8, the desorption process has a similar time scale as the sorption process for the same combination of sediments and sorbate, although desorption is slightly faster because of the smaller averaged particle size for contaminated North River sediments used in the desorption experiment. Both sorption and desorption processes were completed in about 2 days in this case, which strongly supports the argument that the sorption process is reversible.

Comparison of Models. We have fit our experimental data with our retarded/radial diffusion model and the two other box models. The one-box model simply fails to fit the data well (Figure 9). The data shows a more rapid uptake at the beginning followed by a slow approach to equilibrium. The two-box model can be adjusted more closely to the data (Figure 9). However, this is not surprising since there are three fitting parameters involved (the two rate constants, k_1 and k_2 , and the fraction of the total sorption capacity in the rapid-exchange compartment, X_1). In addition, the primary disadvantage of the two-box model is the difficulty of relating these three parameters

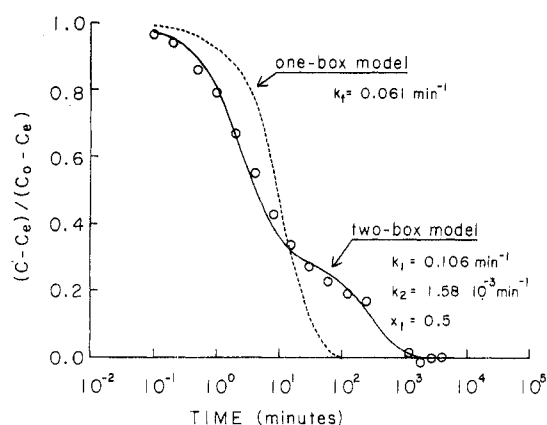


Figure 9. Model-fitting results (for data of experiment 4) with one-box and two-box models.

to known properties of sediments. For example, for two experiments with the same compound (tetrachlorobenzene) and the same sediments (Charles River sediments), however, with different mean aggregate sizes (96 and 232 μm), we obtain two totally different sets of parameters ((1) $k_1 = 5.8 \times 10^{-2} \text{ min}^{-1}$, $k_2 = 2.8 \times 10^{-3} \text{ min}^{-1}$, and $X_1 = 0.44$; (2) $k_1 = 8.7 \times 10^{-3} \text{ min}^{-1}$, $k_2 = 3.2 \times 10^{-4} \text{ min}^{-1}$, and $X_1 = 0.67$) by minimizing the fitting residual. This indicates that we have to experimentally estimate these parameters for each type of sediment, which is impractical for modeling natural water systems. Consequently, these models limit our understanding of the processes governing sorption kinetics and require recalibration for every new situation in which they are applied.

On the contrary, since the particle diameters can be measured, the retarded/radial diffusion model can be fit to the polychlorobenzene uptake data adjusting only one parameter (the effective intraparticle diffusivity). This model fits our results very well (Figure 10a-d). In addition, this model not only extends our understanding of the sorption kinetics but also offers us the opportunity to estimate the effective diffusivity a priori on the basis of correlations with chemical and sediment properties.

Effective Diffusivity, D_{eff} . Table II summarizes the values of the fitting parameter, D_{eff} . According to the previous discussion, the effective diffusivity should be inversely related to the partition coefficient, K_p , for strongly hydrophobic compounds if pore fluid diffusion dominates. Figure 11 shows the relationship of D_{eff} vs. K_p for the various combinations of sorbates and sorbents used. The inverse relationship for these parameters is obvious and consistent with our intraparticle diffusion model. Since the partition coefficient can be estimated from the octanol-water partition coefficient of the compound and the organic carbon content of sediments within a reasonable range (36), the molecular diffusivity can be predicted by the Stokes-Einstein equation (33), and we can measure the particle size distribution and dry solid density, ρ_s , the only factors that we have to know to independently estimate D_{eff} are the porosity and pore geometry factors, $f(n,t)$.

Ullman and Aller (37) related the pore geometry factor to porosity in sediment beds, i.e.

$$f(n,t) = n^i \quad (11)$$

where the exponent, i , is between 1 and 2. If we treat intraparticle diffusion similarly and arbitrarily take i to be 1, the effective diffusivity takes the form:

$$D_{\text{eff}} = \frac{D_m n^2}{K_p (1 - n) \rho_s} \quad (12)$$

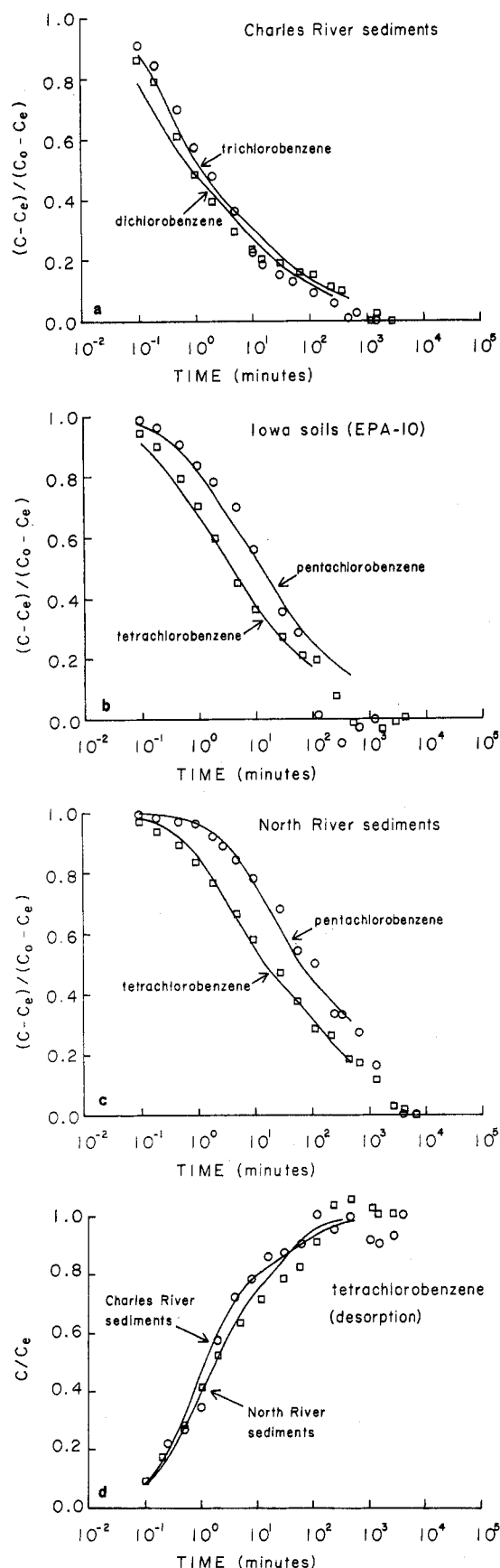


Figure 10. Experimental and model-fitting results for experiments (a) 2 and 3, (b) 9 and 10, (c) 11 and 12, and (d) 13 and 14. Lines are fitting results by retarded/radial diffusion model.

The porosity, n , becomes the only fitting parameter.

We can evaluate what the intraparticle porosities would have to be to yield the observed D_{eff} . The results of this

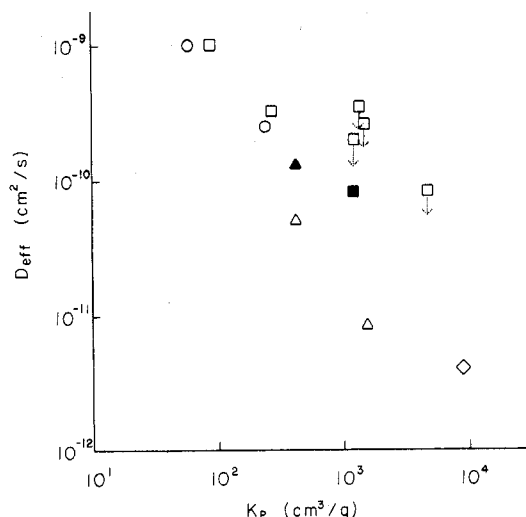


Figure 11. Model fit D_{eff} vs K_p . Squares are data from Charles River sediments, circles are from Iowa soils, and triangles are from North River sediments. Diamonds are data of kepone sorption on Range Point sediments by Connolly (38). Solid symbols represent desorption results from corresponding sorbents. Arrows indicate experiments in which continuous bubbling caused disaggregation and therefore yielded upper limit estimates of D_{eff} .

Table III. Intraaggregate Porosities Which Yield Observed D_{eff} for $i = 1$ (Equation 12)

sediments	compounds	fitting porosity, n
Sorption		
CR ^a	P ^a	(0.32) ^c
CR	TR	0.17
CR	D	0.17
CR	TE	(0.26) ^c
CR	TE (96 μ m)	(0.33) ^c
CR	TE (232 μ m)	(0.39) ^c
IS	TE	0.15
IS	P	0.15
NR	TE	0.09
NR	P	0.07
range point ^b	kepone	0.11
		av 0.13 \pm 0.04
Desorption		
CR	TE	0.18
NR	TE	0.14

^a Same notation as in Table II. ^b Data from ref 38. ^c These values were not used in averaging due to changing particle size distributions during experiments.

evaluation (Table III) show that, for three different types of sediments, the fitting porosity varies by about a factor of 2 (i.e., 0.07–0.17) and is very closely reproduced for any one sediment studied with different sorbates. In light of our physical picture of sorptive exchange, we would predict that the same intraparticle porosity fraction should apply for desorption as for sorption. Indeed, the fitting porosities, n , for desorption of tetrachlorobenzene from Charles River and North River sediments are similar to the values obtained from corresponding uptake experiments. Connolly (38) used a comparable approach to study the sorption of kepone on Range Point sediments (salt marsh, Santa Rosa Sound, FL). He obtained a D_{eff} of 3.7×10^{-12} cm²/s and K_p of 9100 cm³/g. Consequently, we can calculate the value of n to be 0.11, which falls within the range of n from our experiments. If we choose $n = 0.13$ as a typical intraparticle porosity for the sorbing silts of our experiments, all of the observed sorption rates can be fit with reasonable accuracy.

We know of no data appropriate to judge these intraaggregate porosity estimates, yet they appear reason-

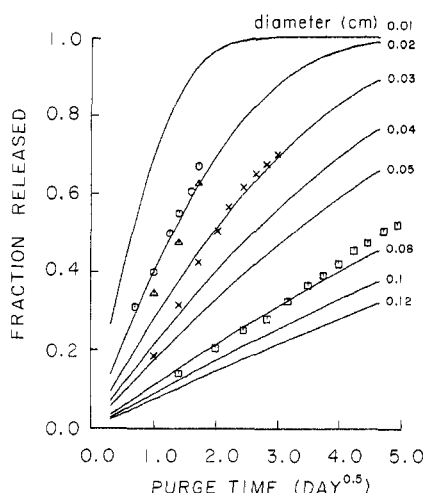


Figure 12. Model prediction compared with desorption experimental results by Karickhoff and Morris (7). The environmental parameters are $i = 1$, $n = 0.13$, $\rho_s = 2.5 \text{ g/cm}^3$, $K_p = 2240 \text{ cm}^3/\text{g}$, and varying diameter. Experimental data were obtained from desorption of hexachlorobenzene from intact pellets (squares), suspended pellets (crosses), crushed pellets (triangles), and parent sediments (circles).

able. Certainly more research is needed to develop methods of characterizing natural aggregate particles and to select key parameters (e.g., n and i) which will enable us to predict a priori the effective diffusivity, D_{eff} , accurately.

Karickhoff and Morris (7) reported the results of desorption of hexachlorobenzene from intact tubificid fecal pellets, suspended pellets, crushed pellets, and parent sediments, separately. Although they reported no data on size distribution, taking n to be 0.13, we can fit their data quite well by adjusting only the averaged particle size in a retarded/radial diffusion model simulations (Figure 12). This analysis indicates that if we know the pellet sizes, our model can fit the shape of their experimental results. In addition, the corresponding "simulation sizes" for intact pellets, suspended pellets, crushed pellets, and parent sediments are 800, 400, 250, and 200 μm , respectively, which appear appropriate for fecal pellets, pellet debris, and silty natural particles.

Applications and Limitations. From the above model analysis it is clear that the radial diffusion sorption kinetics model can be applied to a variety of environmental situations by adjusting the D_{eff} according to easily measured or estimated environmental parameters. Therefore, once it is incorporated in the fate models it will certainly improve our capability to predict the fates of organic pollutants and the related human exposures. In addition, the approximate time scale of sorption and desorption can be easily predicted from analytical solutions to the radial diffusion governing equations if the particle size distribution is sufficiently narrow that we can choose a reasonable average particle size (e.g., method by Rao and co-workers (27) and Cooney and Adesanya 30)). For example, in an open system where desorbed chemicals are flushed away the released fraction of sorbate reaches 50% at a time of $0.03R^2/D_{\text{eff}}$ and reaches 90% at a time of $0.2R^2/D_{\text{eff}}$ (28). Thus, we propose that this model may serve as a useful tool to quickly estimate the mobility of an organic pollutant from an environmental location.

It has been reported that sorptive exchange may require extended times (weeks to months) for complete equilibration (6). On the basis of our retarded/radial diffusive description, this could be due to very long diffusive path lengths and/or high microscale retardation. Limited by the present laboratory setup we have not obtained ex-

perimental results on sorption kinetics with very large soil or sediment particles ($>200 \mu\text{m}$) or with very hydrophobic substances (e.g., $K_{\text{ow}} > 10^5$). However, for silty particles of relatively large mean diameter of 200 μm and f_{oc} of 3%, we would expect hexachlorobenzene to show a desorption time scale of 90% release in about 20 days. Longer sorption time scales will be expected for even more hydrophobic compounds. For instance, polychlorinated biphenyls with octanol-water partition coefficients, K_{ow} , of 10^5 – 10^8 (39) will show time scales of 90% release up to 280 days from particles with a diameter of 50 μm and a few percent organic carbon content. Some additional factors which may also result in this extended sorption time scale include (1) a steric effect in which a large sorbate molecule experiences diminished mobility as some intraparticle pore spaces are too small to pass through, (2) formation of large aggregates and therefore long diffusion path lengths in situations of high sediment concentration, and (3) special pore geometry in some natural particles (e.g., space between expandable clay layers and debris of tissue of dead organisms with very compact structure). More research is needed to shed light on the "highly retarded" sorption process especially based on more understanding on the characteristics of natural particles.

Conclusions

We have used experimental and model simulation approaches to investigate the kinetics of sorption of organic pollutants on natural sediments. Efforts were made to identify the important factors controlling sorption kinetics and to model the process using measurable system parameters based on known physical and chemical processes. Our evidence supports the theory that the sorption kinetics is controlled by intraparticle diffusion for natural aggregated sediments and soils. The results demonstrate that the bigger aggregates have lower uptake rates, that compounds with higher values of K_{ow} show slower sorption, that there is about a factor of 2 effect on sorption kinetics due to variations in K_p in a temperature range of 30 $^{\circ}\text{C}$ (i.e., 25–55 $^{\circ}\text{C}$), and that desorption rates are consistent with a reversible diffusive exchange mechanism. Model simulation analysis indicates that the radial diffusion model is the best among the three tested models because it fits the data as well as the two-box model and much better than the one-box model, and it has only one fitting parameter, the intraparticle diffusivity, rather than three fitting parameters as the two-box model has. The observed effective diffusivity is a function of chemical and particle properties (i.e., $D_{\text{eff}} = D_m n^2 / [K_p (1 - n) \rho_s]$). An empirical choice of $n = 0.13$ could fit all our experimental results and other reported research results with reasonable accuracy. Consequently, this model not only extends our understanding of the sorption kinetics but also enables us to estimate the effective diffusivity a priori on the basis of correlations with chemical and sediment properties.

Acknowledgments

We gratefully acknowledge the guidance and support of Robert Ambrose and Sam Karickhoff during this research program. Additionally, we thank Bruce Brownawell, David Dzombak, and Rene Schwarzenbach for their numerous thoughtful suggestions on the manuscript.

Registry No. P, 608-93-5; TE, 634-66-2; TR, 120-82-1; D, 106-46-7.

Literature Cited

- (1) Kay, B. D.; Elrick, D. E. *Soil Sci.* 1967, 104, 314–322.
- (2) van Genuchten, M. T.; Wierenga, P. J. *Soil Sci. Am. J.* 1976, 40, 473–480.

- (3) Rao, P. S. C.; Davidson, J. M.; Jessup, R. E.; Selim, H. M. *Soil Sci. Soc. Am. J.* 1979, 43, 22-28.
- (4) Schwarzenbach, R. P.; Westall, J. *Environ. Sci. Technol.* 1981, 15, 1360-1367.
- (5) Freeman, D. H.; Cheung, L. S. *Science (Washington, D.C.)* 1981, 214, 790-792.
- (6) Karickhoff, S. W. *J. Hydraul. Eng.* 1984, 110, 707-735.
- (7) Karickhoff, S. W.; Morris, K. R. *Environ. Sci. Technol.* 1985, 19, 51-56.
- (8) Onishi, Y.; Wise, S. E. *Mathematical Model, SERATRA, For Sediment-Contaminant Transport In River and Its Application to Pesticide Transport in Four Mile and Wolf Creeks in Iowa*; U.S. Environmental Protection Agency: Athens, GA, 1982; EPA-600/3-82-045, p 7.
- (9) Ambrose, R. B., Jr.; Hill, S. S.; Mulkey, L. A. *User's Manual for The Chemical Transport and Fate Model TOXIWASP Version 1*; U.S. Environmental Protection Agency: Athens, GA, 1983; EPA-600/3-83-005, p 13.
- (10) Lapidus, L.; Amundson, N. R. *J. Phys. Chem.* 1952, 56, 984-988.
- (11) Oddson, J. K.; Letey, J.; Weeks, L. V. *Soil Sci. Soc. Am. Proc.* 1970, 34, 412-417.
- (12) Karickhoff, S. W. In *Contaminants and Sediments: Analysis, Chemistry, and Biology*; Baker, R. A., Ed.; Ann Arbor Science: Ann Arbor, MI, 1980; Vol. 2, pp 193-205.
- (13) Leenheer, J. A.; Ahlrichs, J. L. *Soil Sci. Soc. Am. J.* 1971, 35, 700-704.
- (14) Hendricks, D. W.; Kuratti, L. G. *Water Res.* 1982, 16, 829-837.
- (15) Chase, R. R. P. *Limnol. Oceanogr.* 1979, 24, 417-426.
- (16) Zabawa, C. F. *Science (Washington, D.C.)* 1978, 202, 49-51.
- (17) Johnson, R. G. *J. Mar. Res.* 1974, 32, 313-330.
- (18) Stevenson, F. J. *Humus Chemistry, Genesis, Composition Reactions*; Wiley: New York, 1982, p 374.
- (19) Brady, N. C. *The Nature and Properties of Soil*, 8th ed.; Macmillan: New York, 1974; p 58.
- (20) Black, C. A.; Evans, D. D.; White, J. L.; Ensminger, L. E.; Clark, F. E. *Methods of Soil Analysis: No. 9 in the Series Agronomy*; American Society of Agronomy: Madison, WI, 1965; p 1367.
- (21) Mathews, A. P.; Weber, W. J., Jr. *Am. Inst. Chem. Eng., Symp. Ser.* 166, 1976, 43, 91-98.
- (22) Prasher, B. D.; Ma, Y. H. *Am. Inst. Chem. Eng. J.* 1977, 23, 303-311.
- (23) Sudo, Y.; Misic, D. M.; Suzuki, M. *Chem. Eng. Sci.* 1978, 33, 1287-1290.
- (24) Weber, W. J., Jr.; Liu, K. T. *Chem. Eng. Commun.* 1980, 6, 49-60.
- (25) Karger, B. L.; Snyder, L. R.; Horvath, C. *An Introduction to Separation Science*; Wiley: New York, 1973; p 80-1.
- (26) Rao, P. S. C.; Jessup, R. E.; Rolston, D. E.; Davidson, J. M.; Kilcrease, D. P. *Soil Sci. Soc. Am. J.* 1980, 44, 684-688.
- (27) Rao, P. S. C.; Jessup, R. E.; Addiscott, T. M. *Soil Sci.* 1982, 133, 342-349.
- (28) Crank, J. *The Mathematics of Diffusion*, 2nd ed.; Clarendon: Oxford, England, 1975; p 93.
- (29) Gschwend, P. M.; Wu, S. C. *Environ. Sci. Technol.* 1985, 19, 90-96.
- (30) Cooney, D. O.; Adesanya, B. A. *Chem. Eng. Sci.* 1983, 38, 1535-1541.
- (31) Gschwend, P. M.; Madsen, O. S.; Wu, S. C.; Wilkin, J. L.; Ambrose, R. B. "Mass Transport of Toxic Chemicals Between Bed and Water," U. S. Environmental Protection Agency, Technical Report. 1985, In preparation.
- (32) Chiou, C. T. *Environ. Sci. Technol.* 1985, 19, 57-62.
- (33) Satterfield, C. N. *Mass Transfer in Heterogeneous Catalysis*; Robert E. Krieger Publishing: Huntington, NY, 1981; p 18.
- (34) Moore, W. J. *Physical Chemistry*, 3rd ed.; Prentice-Hall: Englewood Cliffs, NJ, 1962; p 180.
- (35) Chiou, C. T.; Porter, P. E.; Schmedding, D. W. *Environ. Sci. Technol.* 1983, 17, 227-231.
- (36) Karickhoff, S. W.; Brown, D. S.; Scott, T. A. *Water Res.* 1979, 13, 241-248.
- (37) Ullman, W. J.; Aller, R. C. *Limnol. Oceanogr.* 1982, 27, 552-556.
- (38) Connolly, J. P. Ph.D. Dissertation, University of Texas at Austin, 1980.
- (39) Rapaport, R. A.; Eisenreich, S. J. *Environ. Sci. Technol.* 1984, 18, 163-170.

Received for review August 29, 1985. Accepted January 21, 1986.
This work was supported by U.S. EPA Contract CR 810472-01-0.

Safe Handling of Chemical Toxicants and Control of Interferences in Human Tissue Analysis for Dioxins and Furans

Louls R. Alexander, Donald G. Patterson,* Gary L. Myers, and James S. Holler

Division of Environmental Laboratory Sciences, Center for Environmental Health, Centers for Disease Control, U.S. Public Health Service, U.S. Department of Health and Human Services, Atlanta, Georgia 30333

■ The development of a comprehensive analytical program in ultratrace analyses of toxic substances requires a facility specifically devoted to synthesis activities and for making analytical standards. The development of adequate operational procedures for such a facility is described. Environmental monitoring is a key activity in protecting the laboratory worker and the analytical integrity of ongoing studies. A wipe test procedure is described that provides the information needed to pinpoint sources of contamination. Examples of operational problems and remedial actions are described for the development of a parts per trillion dioxin analytical method.

Introduction

During the last 2 years, the Division of Environmental Laboratory Sciences, formerly the Clinical Chemistry

Division, Center for Environmental Health, Centers for Disease Control (CDC), has been developing the capability for accurately and precisely measuring 2,3,7,8-tetrachlorodibenzo-*p*-dioxin (TCDD) and the other TCDD isomers in human tissue samples while at the same time synthesizing dioxins and furans for use as analytical standards (1). Any laboratory conducting work with dioxins should have (1) facilities designed to safely handle such hazardous materials and (2) adequate safety guidelines (2). To facilitate the safe handling of these dioxins, CDC has established a Chemical Toxicant Laboratory (CTL) facility (see Figure 1) that permits work on limited quantities of these compounds. Briefly, some of the features of this laboratory include the following: an isolated laboratory quadrant; limited access; separate dressing room facilities; shower/toilet facilities; a seamless vinyl floor; a pass-through compartment; view windows; stainless steel